PHYSICAL REVIEW B **83**, 161302(R) (2011)

Defect-dominated diameter dependence of fracture strength in single-crystalline ZnO nanowires: *In situ* experiments

Mo-Rigen He and Jing Zhu*

Beijing National Center for Electron Microscopy, Laboratory of Advanced Materials, Department of Materials Science and Engineering, Tsinghua University, Beijing 100084, China

(Received 24 January 2011; published 18 April 2011)

Diameter (D) dependence of fracture strength in [0001]-oriented single-crystalline ZnO nanowires (NWs) with D ranging from 18 to 114 nm is experimentally revealed via *in situ* uniaxial tension. The lower bound of the scattered strengths increases with decreasing D, following a modified power law, and critical defects that effectively dominate the strengths are attributed to the diameter-dependent quantities of discrete point defects in NWs, based on *in situ* cathodoluminescence spectra. As a result, the size-effect mechanism of fracture strength is well understood, accounting for a simple and basic case of single-crystalline NWs.

DOI: 10.1103/PhysRevB.83.161302 PACS number(s): 62.20.mm, 62.25.Mn

Due to the unique combination of piezoelectric, semiconducting, and biocompatible properties,[1] ZnO nanowires (NWs) are recognized as promising candidates for various nanoelectromechanical devices, such as generators,[2] resonators,[3] and force sensors,[4] which call for NWs capable of sustaining extreme external loadings. Therefore, understanding the mechanical properties of NWs, especially their fracture strengths σ_{FS}, is essential for optimizing the reliability and performance of these devices.

Since the 1920s,[5] there has been wide concern that σ_{FS}, dominated by so-called *critical defects*, increase with the decrease of the characteristic sizes of specimens, and, in nanoscale, such size effect of σ_{FS} is attracting increasing interest. Experimental techniques for *in situ* bending[6–8] and tensile testing[9–11] have been recently developed, based on which the σ_{FS} in ZnO NWs were evaluated. For instance, Wen *et al*. reported a linear relationship between σ_{FS} and NW diameters (D);[8] others also reported monotonically increasing σ_{FS} with decreasing D.[9,11] However, such size effects have not yet been quantitatively modeled based on, for example, the fracture mechanics of diameter-dependent critical defects. By contrast, Agrawal *et al*. presented a range of remarkably scattered σ_{FS}, which were attributed to surface defects,[10] but they did not probe into the size effect of σ_{FS}.

In our previous work,[12] Young's moduli (YM) in ZnO NWs were measured via *in situ* uniaxial tension in a scanning electron microscope (SEM). Here we utilize the same method to study the diameter dependence of σ_{FS} in ZnO NWs, and *in situ* cathodoluminescence (CL) characterizations are further performed to reveal the underlying microstructural mechanism.

Single-crystalline ZnO NWs were synthesized as reported before,[13] with uniform diameter along the [0001]-axis and atomic-level clean $\{10\bar{1}0\}$ side surfaces [see Figs. 1(a) and 1(b)]. Uniaxial tensile testing of the as-synthesized NWs was carried out *in situ* using our homemade system [see Fig. 1(c)] in SEM (JSM-6301F, JEOL). Prior to testing, two ends of an individual NW were respectively glued onto the tungsten tip and the loading cantilever [see Fig. 1(d)], and the NW axis was aligned with the direction of tensile load according to procedures described elsewhere.[12] Then, stresses (σ) were stepwise applied to the NW by the nanopiezomotor and were calculated from deflection of the loading cantilever [see Fig. 2(a)]. Strains (ε) were measured between the two reference points on the NW, thus eliminating the error owing to the slippage between the NW and tips.[14]

Thereby, σ-ε curves were measured for ZnO NWs with D ranging from 18 to 114 nm, as demonstrated in Fig. 2(b). Each NW sample deformed linear-elastically throughout testing and finally fractured in a typical brittle manner, leaving a cleavage plane perpendicular to the [0001]-axis. Thus, σ_{FS} could be easily determined from the σ-ε curve and its diameter dependence was experimentally revealed (see Fig. 3).

The measured σ_{FS} in NWs lay in 3–13 GPa, far larger than the bulk value, which is typically smaller than 200 MPa.[15] For D larger than about 50 nm, σ_{FS} were remarkably scattered, manifesting the defect-dominated nature that strengths of NWs are not determined uniquely by their size parameters, unlike their diameter-dependent YM.[12] Nonetheless, increasing of the scattered σ_{FS} became notable as D decreased to <50 nm, clearly revealing the size effect, and the σ_{FS} as large as 13 GPa preceded all those reported in ZnO NWs until now.[6–11] (Although fracture strains as large as 15% have been reported,[9] the corresponding YM of $\sim$20 GPa were quite lower than the recognized value). Qualitatively, this significant strengthening resulted from the reduction of critical defects, and Fig. 1(b) shows that because as-synthesized NWs have such perfectly flat surfaces, evident surface flaws[9] are not observed yet in our transmission electron microscopy (TEM) characterizations. Furthermore, the large amount of measurements enabled us to extract the size effect of σ_{FS} from the rather scattered experimental results.

The concept of size-dependent reduction of critical defects has been widely quoted to explain the diameter dependence of σ_{FS} in NWs,[8,11] however, without further quantitative discussion. Meanwhile, for quasibrittle fracture of specimens ranging from the macrometer to micrometer scale, a rather similar assumption, i.e., critical defect sizes are proportional to specimen sizes (D), leads to Bažant's size effect of σ_{FS}, which is written as[16]

$$\sigma_{FS}(D) = \sigma_0 \left(1 + \frac{D}{D_0}\right)^{-1/2}, \tag{1a}$$

where the constants σ_0 and D_0 are determined by both the ideal strength and the size of fracture process zone (FPZ) comparable to D.[16] As Fig. 3 shows, this classic scaling law agrees with the experimental data merely in that σ_{FS} increase

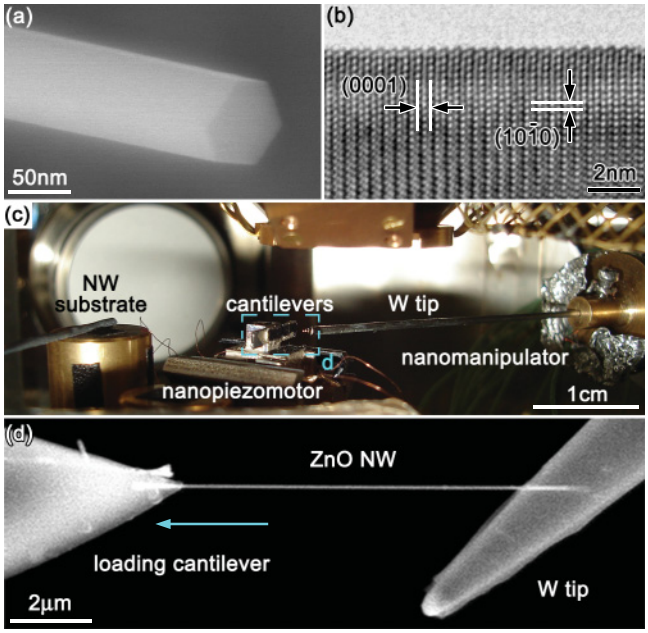

FIG. 1. (Color online) (a) SEM image showing the hexagonal cross section, and (b) high-resolution TEM (JEM-2010F, JEOL) image showing the atomic-level flat {10$\bar{1}$0} side surfaces of the [0001]-oriented ZnO NWs. (c) *In situ* mechanical testing system consisting of a tungsten tip on the nanomanipulator and a pair of cantilevers (with force constant K) carried on the nanopiezomotor (Ref. 12). (d) ZnO NW undergoing uniaxial tension, direction indicated by the arrow.

with decreasing D, but the steepness of increasing σ_{FS} is quite underestimated in the fitting, probably because there are few defects, and thus critical defects (i.e. effective cracks) cannot be sufficiently formed, in NWs corresponding to the upper-bound of σ_{FS}. Nonetheless, fitting the lower bound using Eq. (1a) is also far from satisfactory.[17]

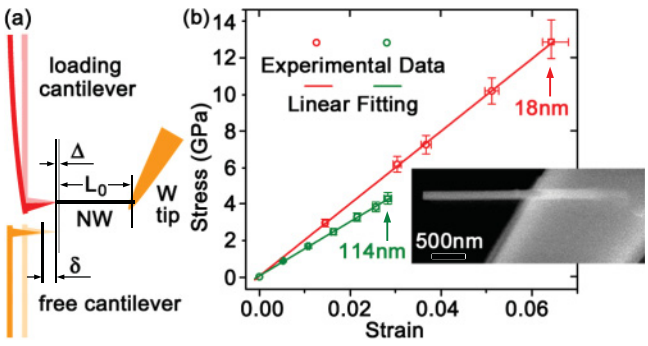

FIG. 2. (Color online) (a) Schematic of a snapshot during testing, based on which the stress ($\sigma = 4K\delta/\pi D^2$) and strain ($\varepsilon = \Delta L_0$) are calculated (Ref. 12). Light-colored cantilevers and reference lines correspond to the initial state. (b) σ-ε curves for ZnO NWs with D=18 nm (red) and 114 nm (green); σ_{FS} are indicated by arrows. (Inset) Morphology of a fractured NW showing the (0001) cleavage plane.

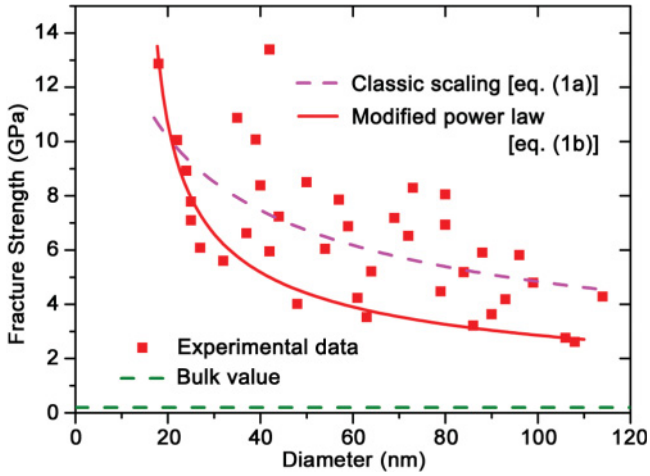

FIG. 3. (Color online) Experimental data (solid squares) for the diameter dependence of σ_{FS} and the fitting using Eq. (1a) (dashed curve). Lower bound of σ_{FS} are fitted using Eq. (1b) (solid curve). Dashed line (green) shows typical σ_{FS} in bulk ZnO (Ref. 15).

In contrast, we found the following modified scaling law works quite well for the lower bound of σ_{FS} (see Fig. 3):

$$\sigma_{FS}(D) = \sigma_0 \left(1 + \frac{D - D_C}{D_0}\right)^{-1/2}, \qquad \text{(1b)}$$

where $\sigma_0 = 17.6$ GPa, $D_0 = 2.3$ nm, and a new characteristic size, $D_C = 16$ nm, are obtained from fitting. Since $D_C > D_0$, Eq. (1b) is truly a different type of scaling other than Eq. (1a), and σ_0 is close to the ideal strength of ZnO at ~14 GPa, i.e. 10% of the bulk YM,[18] implying that the size of FPZ is in atomic-scale. Thus, we revealed that the lower bound of σ_{FS} in single-crystalline NWs can also be described with a modified power law.

As an analogy to Bažant's classic power law, the applicability of Eq. (1b) indicates that the upper bound of critical defect size scales with (D–D_C); now we discuss this size effect from the perspective of real microstructural defects in the tested ZnO NWs. First, to the best of our knowledge, volume-extended (i.e., planar) defects and evident surface flaws have not been found yet to the extent of TEM characterizations. One should note that the TEM samples were not the very mechanically-tested NWs (since *in situ* tensile testing was not performed in TEM), although it is straightforward to regard the former to be representative of the latter. We thus assumed that planar and surface defects can be excluded from the following discussion. Moreover, the effects of electron-beam irradiation that are of great concern, i.e., depressing the strength and enhancing the ductility of NWs,[19] can also be ruled out for *in situ* SEM experiments, since the ~5-kV e-beam is too weak in energy to introduce point defects.[17] Therefore, it is highly probable that native point defects dominate in the as-synthesized and tested NWs. Specifically, the oxygen and zinc ionic vacancies with lower formation energies are the most expected intrinsic defects in ZnO, by the extensive first-principles calculations.[20]

The existence of point defects in NWs was confirmed by *in situ* CL experiments. ZnO NWs were transferred from the substrate onto a copper grid and observed under SEM (Quanta 200F, FEI) using an e-beam voltage of 15 kV. CL spectra for

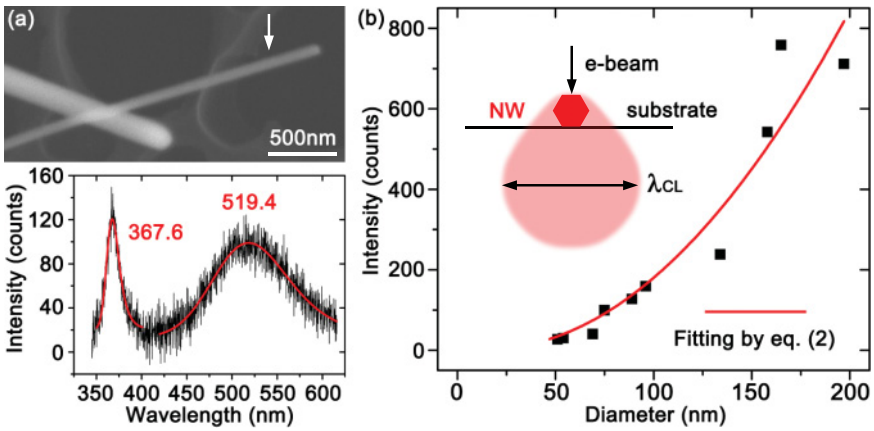

FIG. 4. (Color online) (a) Morphology and CL spectrum of a typical ZnO NW with $D = 75$ nm; arrow indicates incident point of e-beam. (b) Experimental results (squares) and modeling (curve) of the diameter-dependent intensities of defect peak. Inset shows relative sizes between NW and CL sampling volume.

individual NWs were acquired from the middle point across the NW diameter via a MonoCL 3+ (Gatan) system. The collection time was 4 s, and the wavelength was scanned from 345 to 615 nm. As shown in Fig. 4(a), CL spectra of the tested ZnO NWs typically consist of the ultraviolet (UV) peak centered at ~368 nm and the green broadband centered at ~519 nm, and it has been well known that the former originates from near-band-edge emission, while the latter, i.e., the "defect peak," is attributed to the electron-hole recombination near the oxygen vacancies (V_O^+).[21] Other point defects, such as V_{Zn}^-, have also been proposed to be the luminescence center.[22]

Furthermore, in Fig. 4(b) we revealed the diameter-dependent intensity of the defect peak $I_{def}(D)$ measured in NWs, with D ranging from 51 to 197 nm (CL signals became undetectable for $D < 50$ nm). As recognized in the literature,[21,23] a linear relationship between $I_{def}(D)$ and the concentration of point defects $C(D)$ has been developed for lightly doped semiconductors, where $C(D) = C_0 \exp(-\Delta p \Omega / k_B T)$ is given by the Young-Laplace equation. Here, C_0 is the intrinsic defect concentration in bulk materials, Ω is volume of the Zn^{2+} and O^{2-} vacancies, $k_B T$ is Boltzmann's factor, and $\Delta p = 2\tau/D$ (τ is the circumferential component of surface tension in $\{10\bar{1}0\}$ side surfaces). Besides, for the 15-kV e-beam incident on bulk ZnO, the beam-broadening due to multiple scattering is ~200 nm, which is the length scale (λ_{CL}) of the sampling volume for CL spectrum.[24] Thus, for ZnO NWs with D smaller than this, it is reasonable to suppose that the whole cross section of the NW contributed to the intensity of CL signals, as illustrated in the inset of Fig. 4(b). After all, $I_{def}(D)$ can be related with the total quantities of point defects $Q(D)$ in a simple form:

$$I_{def}(D) = I_0 \nu Q(D) = I_0 \nu \lambda_{CL} D^2 C(D) = A D^2 \exp\left(-\frac{2D_C}{D}\right). \quad (2)$$

Here, I_0 is the intensity of incident e-beam, controlled by experimental parameters such as beam current, spot size, and defocus, and ν is excitation efficiency of the defect peak. Thus, A is considered a constant for the NWs measured under identical conditions, and $D_C = \tau\Omega/k_B T$. The effect of point defect concentration in Eq. (2), i.e., the exponent term, was also supported by measuring the intensity of the near-band-edge emission $I_{NBE}(D)$ and the ratio I_{def}/I_{NBE}, in which the effect of sample volume (the D^2 term) can be eliminated.[17]

As found in Fig. 4(b), the experimental $I_{def}(D)$ is well described by Eq. (2). Moreover, expanding Eq. (2) with D approximately gives $Q(D) \propto (D - D_C)^2$, and the D_C=15.7 nm yielded from fitting agrees quantitatively well with the D_C=16.0 nm given by Eq. (1b). Therefore, the size-dependent reduction of the upper bound of critical defect sizes, i.e., $\propto (D - D_C)$, can be straightforwardly understood on condition that it scales with the square root of $Q(D)$. This assumption means that all the native point defects in NWs are involved in dominating their minimum strengths via some kinds of "combination effects," such as stress concentrations and defect aggregations, which have been indicated in previous atomistic simulations.[25] Thus, a microstructural mechanism based on the diameter-dependent quantities of point defects is obtained for the scaling law of the lower bound of σ_{FS}. And, more generally, the stochastic quantity of the "combined" point defects experimentally leads to the scattering of σ_{FS}.

Yet, we still need to state that the preparation and manufacturing processes as well as the detailed microstructures of NWs also play important roles in their fracture and strength properties. For instance, strengths could be far lower than theoretical values in cases where they are dominated by nonequilibrium extended defects such as stacking faults, twin boundaries, and surface roughness,[26] and their size effect would therefore be more difficult to depict in a concise scaling law.

In summary, based on *in situ* SEM tensile testing combined with CL spectra, the size effect of σ_{FS} in ZnO NWs are experimentally related to the diameter-dependent quantities of discrete point defects, and a modified power-form scaling law is presented for the lower bound of σ_{FS}. Although the model shown here accounts for a very simple case of single-crystalline NWs, it should be the basis for a full understanding of the strength properties in nanoscale.

We thank Jun Xu of Peking University for help in CL experiments and Aijun Tong of Tsinghua University for analyses of CL spectra. The experiments made use of the resources of the Beijing National Center for Electron Microscopy. This work was financially supported by the National 973 Project of China (2009CB623700) and National Natural Science Foundation of China (50831001).

*Corresponding author: jzhu@mail.tsinghua.edu.cn

[1]Z. L. Wang, J. Phys. Condens. Matter **16**, R829 (2004).

[2]Z. L. Wang and J. H. Song, Science **312**, 242 (2006).

[3]X. D. Bai, P. X. Gao, Z. L. Wang, and E. G. Wang, Appl. Phys. Lett. **82**, 4806 (2003).

[4]X. D. Wang, J. Zhou, J. H. Song, J. Liu, N. S. Xu, and Z. L. Wang, Nano Lett. **6**, 2768 (2006).

[5]A. A. Griffith, Philos. Trans. R. Soc. London, Ser. A **221**, 163 (1921).

[6]C. Q. Chen and J. Zhu, Appl. Phys. Lett. **90**, 043105 (2007).

[7]S. Hoffmann, F. Östlund, J. Michler, H. J. Fan, M. Zacharias, S. H. Christiansen, and C. Ballif, Nanotechnology **18**, 205503 (2007).

[8]B. M. Wen, J. E. Sader, and J. J. Boland, Phys. Rev. Lett. **101**, 175502 (2008).

[9]A. V. Desai and M. A. Haque, Sens. Actuators A **134**, 169 (2007).

[10]R. Agrawal, B. Peng, and H. D. Espinosa, Nano Lett. **9**, 4177 (2009).

[11]F. Xu, Q. Q. Qin, A. Mishra, Y. Gu, and Y. Zhu, Nano Res. **3**, 271 (2010).

[12]M. R. He, Y. Shi, W. Zhou, J. W. Chen, Y. J. Yan, and J. Zhu, Appl. Phys. Lett. **95**, 091912 (2009).

[13]Y. S. Zhang, L. S. Wang, X. H. Liu, Y. J. Yan, C. Q. Chen, and J. Zhu, J. Phys. Chem. B **109**, 13091 (2005).

[14]R. Agrawal, B. Peng, E. E. Gdoutos, and H. D. Espinosa, Nano Lett. **8**, 3668 (2008).

[15]C. S. Lu, R. Danzer, and F. D. Fischer, Phys. Rev. E **65**, 067102 (2002).

[16]Z. P. Bažant, Proc. Natl. Acad. Sci. USA **101**, 13400 (2004).

[17]See supplemental material at [http://link.aps.org/supplemental/10.1103/PhysRevB.83.161302] for (i) detailed results on fitting the lower bound of σFS using Eq. (1a), (ii) further TEM characterization of ZnO NWs, (iii) discussions on the e-beam irradiation effects, and (iv) diameter dependence of the ratio I_{def}/I_{NBE}.

[18]I. B. Kobiakov, Solid State Commun. **35**, 305 (1980).

[19]N. W. Moore, J. H. Luo, J. Y. Huang, S. X. Mao, and J. E. Houston, Nano Lett. **9**, 2295 (2009); J. H. Luo, F. F. Wu, J.Y. Huang, J. Q. Wang, and S. X. Mao, **104**, 215503 (2010).

[20]A. F. Kohan, G. Ceder, D. Morgan, and C. G. Van de Walle, Phys. Rev. B **61**, 15019 (2000); P. Erhart, K. Albe, and A. Klein, *ibid*. **73**, 205203 (2006).

[21]K. Vanheusden, W. L. Warren, C. H. Seager, D. R. Tallant, J. A. Voigt, and B. E. Gnade, J. Appl. Phys. **79**, 7983 (1996); A. van Dijken, E. A. Meulenkamp, D. Vanmaekelbergh, and A. Meijerink, J. Lumin. **90**, 123 (2000).

[22]X. L. Wu, G. G. Siu, C. L. Fu, and H. C. Ong, Appl. Phys. Lett. **78**, 2285 (2001).

[23]B. G. Yacobi and D. B. Holt, *Cathodoluminescence Microscopy of Inorganic Solids*, 1st ed. (Plenum, New York, 1990).

[24]X. B. Han, L. Z. Kou, X. L. Lang, J. B. Xia, N. Wang, R. Qin, J. Lu, J. Xu, Z. M. Liao, X. Z. Zhang, X. D. Shan, X. F. Song, J. Y. Gao, W. L. Guo, and D. P. Yu, Adv. Mater. (Weinheim, Ger.) **21**, 4937 (2009).

[25]W. F. Zhou, G. T. Fei, X. F. Li, S. H. Xu, L. Chen, B. Wu, and L. D. Zhang, J. Phys. Chem. C **113**, 9568 (2009); A. Adnan and C. T. Sun, J. Mech. Phys. Solids **58**, 983 (2010).

[26]M. J. Gordon, T. Baron, F. Dhalluin, P. Gentile, and P. Ferret, Nano Lett. **9**, 525 (2009).